



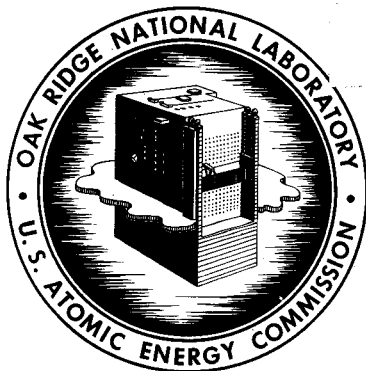
3 4456 0443711 6

CENTRAL RESEARCH LIBRARY
DOCUMENT COLLECTION

ORNL-3552
UC-25 - Metals, Ceramics, and Materials
TID-4500 (26th ed.)

X-RAY MASS ATTENUATION COEFFICIENTS IN THE
RANGE OF 50 TO 150 kvp WITH DATA FOR
SEVERAL REACTOR MATERIALS

B. E. Foster
J. W. Evans



OAK RIDGE NATIONAL LABORATORY
operated by
UNION CARBIDE CORPORATION
for the
U.S. ATOMIC ENERGY COMMISSION

LEGAL NOTICE

This report was prepared as an account of Government sponsored work. Neither the United States, nor the Commission, nor any person acting on behalf of the Commission:

- A. Makes any warranty or representation, expressed or implied, with respect to the accuracy, completeness, or usefulness of the information contained in this report, or that the use of any information, apparatus, method, or process disclosed in this report may not infringe privately owned rights; or
- B. Assumes any liabilities with respect to the use of, or for damages resulting from the use of any information, apparatus, method, or process disclosed in this report.

As used in the above, "person acting on behalf of the Commission" includes any employee or contractor of the Commission, or employee of such contractor, to the extent that such employee or contractor of the Commission, or employee of such contractor prepares, disseminates, or provides access to, any information pursuant to his employment or contract with the Commission, or his employment with such contractor.

ORNL- 3552

Contract No. W-7405-eng-26

Metals and Ceramics Division

X-RAY MASS ATTENUATION COEFFICIENTS IN THE RANGE OF
50 TO 150 kvp WITH DATA FOR SEVERAL REACTOR MATERIALS

B. E. Foster and J. W. Evans

FEBRUARY 1964

OAK RIDGE NATIONAL LABORATORY
Oak Ridge, Tennessee
operated by
UNION CARBIDE CORPORATION
for the
U. S. ATOMIC ENERGY COMMISSION



3 4456 0443711 6

•

•

•

•

•

•

•

•

X-RAY MASS ATTENUATION COEFFICIENTS IN THE RANGE OF
50 TO 150 kvp WITH DATA FOR SEVERAL REACTOR MATERIALS

B. E. Foster and J. W. Evans¹

ABSTRACT

Experimental determinations of the low-energy x-ray attenuation coefficients of some materials associated with nuclear technology were made to permit their use in homogeneity studies and various radiographic techniques.

The materials examined were types 304 and 347 stainless steel, Zircaloy-2, type 1100 aluminum, and uranium-aluminum alloys of 7, 18, and 25 wt % U.

All attenuation coefficients determined were narrow-beam coefficients. To prevent the detection of any photon that experienced a large deflection angle, the x-ray beam was finely collimated; as a part of the collimation, the detector was well shielded and located far from the absorber.

A Norelco 150 x-ray unit was used as the source of radiation. The detector was a thallium-activated NaI crystal, optically coupled to a photomultiplier tube. The equipment, its operation, and the experimental procedure are discussed in detail.

Experimental calculations were based on Lambert's law as applied to x rays. Theoretical coefficients were based on reported data. Mass attenuation coefficients were determined as the summation of the fractional absorption caused by the significant constituent elements within the limits of predetermined energy ranges.

INTRODUCTION

There has been an increasing interest in x-ray absorption properties of materials, particularly in the field of nondestructive testing. This interest arises from the direct use of x-ray absorption for the measurement of homogeneity, density, or thickness of materials. The current absorption information is restricted to theoretical x-ray attenuation

¹Presently with General Electric Company, Cincinnati, Ohio.

coefficients on particular elements, with a computer extrapolation for those remaining elements. Experimental data on specific alloys are not generally available. Therefore, a research program was begun to experimentally determine the x-ray absorption coefficients of alloys associated with nuclear technology.

The purpose of the investigation was to measure, as a function of energy, the x-ray attenuation coefficients of specific alloys. These results may be applied to the alloys studied for the gaging of thickness, the determination of density, and/or the measurement of homogeneity. The material selection was based on the necessity for this information in nuclear reactor technology. The materials examined were types 304 and 347 stainless steel, 1100 aluminum, Zircaloy-2, and enriched (93% U^{235}) uranium-aluminum alloys containing 7.0, 18.6, and 24.8 wt % U. Energy boundary conditions of 40 to 130 kev were dictated by the capacity and range of the Norelco (50 to 150 kvp) x-ray unit employed.

Theory

A review of the literature reveals that considerable effort has been devoted to fundamental x-ray absorption coefficients for the elements. G. W. Grodstein² has calculated coefficients for 24 elements. Grodstein's calculations were based on the probabilities of the various interactions taking place within matter when it is subjected to electromagnetic radiation. E. Storm, E. Gilbert, and H. Israel³ did additional work on element absorption when they extrapolated, with the aid of an IBM 704 computer, the homogeneous x-ray absorption coefficients for elements 1 through 100 from the 19 elements computed by G. R. White.⁴

²G. W. Grodstein, "X-Ray Attenuation Coefficients from 10 kev to 100 Mev," Nat. Bur. Std. (U.S.) Circ. 583, Washington, D. C. (1957).

³E. Storm, E. Gilbert, and H. Israel, Gamma Ray Absorption Coefficients for Elements 1 through 100 Derived from the Theoretical Values of the National Bureau of Standards, LA-2237, Los Alamos Scientific Laboratory (1958).

⁴G. R. White, "X-Ray Attenuation Coefficients from 10 kev to 100 Mev," Nat. Bur. Std. (U.S.) Rept. 1003, Washington, D. C. (1952).

The events which take place within an absorber when subjected to low-energy quanta (less than 1 mev) include the photoelectric effect, the Compton effect, coherent scattering, and secondary fluorescent emission. These interactions have been thoroughly discussed by Clark⁵ and Compton.⁶ The total attenuation of photons is a summation of the interactions of these various quanta with matter. This is graphically illustrated according to B. E. Dozer⁷ in Fig. 1, where the total attenuation coefficient curve for tin is the result of the absorption due to photoelectric effect, Compton effect, and pair production. As expected, the predominant contributing event at low energies is the photoelectric effect.

Equipment

The energy range of 0-150 kvp (0-130 kev) was of primary interest, and for this reason use was made of a Norelco 150 x-ray unit.

Different numbers of copper filters, in increments of 100-mil thickness, were placed in the x-ray beam to reduce the beam intensity with a high tube amperage to available photomultiplier tolerances. The high tube amperage was necessary to improve stability of the x-ray beam. In addition, the filters served to harden the x-ray beam, thus causing the x-ray spectral peak to be sharper and enabling more accurate location of this peak with the detection and counting system.

The detection method, which employed a sodium-iodide crystal and photomultiplier tube, was selected on the basis of three major considerations. These were (a) linearity of the detector output throughout the energy range used, (b) high detection efficiency, and (c) resolving time which would allow a high-duty cycle without severe dead-time losses. All of these features were characteristic of the scintillator-photomultiplier method. A $3 \times 1 \frac{1}{2}$ -in. crystal of sodium iodide (thallium activated) optically

⁵G. L. Clark, Applied X-Rays, McGraw-Hill, New York, 1940.

⁶A. H. Compton and S. K. Allison, X-Rays in Theory and Experiment, D. Van Nostrand Co., Inc., New York, 1957.

⁷B. E. Dozer, A Null Balance X-Ray Absorption Instrument for Chemical Process Monitoring, HW-60898, Hanford Atomic Products Operation (1959).

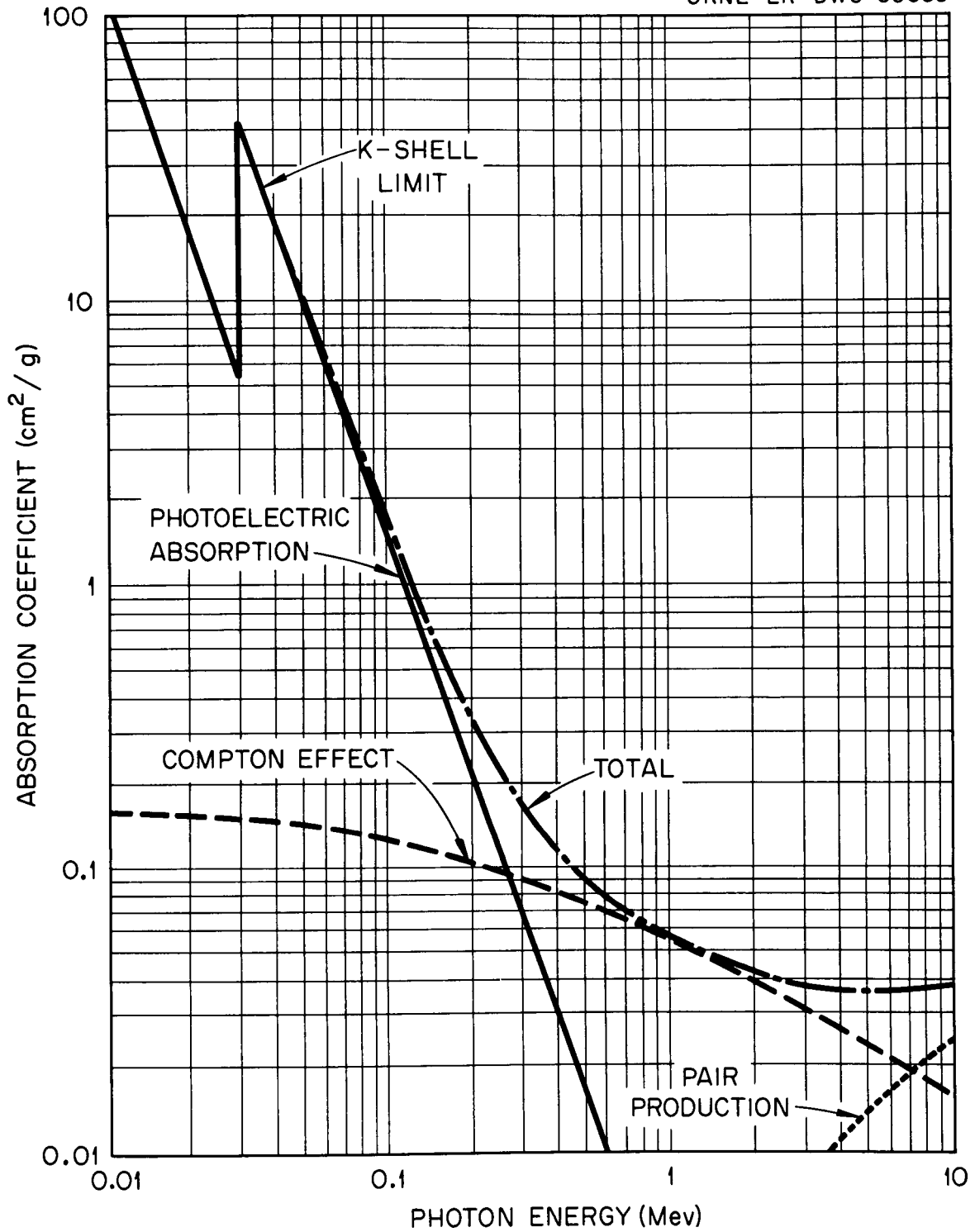


Fig. 1. Absorption Coefficients for Tin.

coupled to a 6363 Du Mont photomultiplier tube was used as the detector head. A smaller crystal and different photomultiplier tube could have been used equally as well.

The selection of the particular linear amplifier and pulse-height selector was based on the needs for low-drift rate over long periods of time and the ability to discriminate between energetic components near the desired spectrum. The double-differentiated amplifier (DD2) which was designed for use with sodium-iodide (thallium activated) detectors fulfilled these requirements. Fairstein⁸ provides a complete technical discussion of the design and capabilities of this amplifier.

The remaining pieces of equipment were of logical selection since the need was for rapid indications of counting rates integrated over a short period of time. For this purpose, the linear count-rate meter and Brown recorder were sufficient. A photograph of the detection system and x-ray control panel is shown in Fig. 2.

The sample materials were selected according to their availability and their applicability to both power- and research-type reactors. The range of sample thickness was based on theoretically approximated attenuation coefficients to give a more uniform intensity change for each sample through the anticipated range of x-ray energies. This control of sample thickness was necessary to achieve the optimum sensitivity and accuracy. Attenuation coefficients for each sample thickness were determined by the summation of the fractional absorption caused by the significant constituent elements within the limits of the predetermined energy levels. Precise values of each of the constituent elements were determined by a chemical analysis with a $\pm 1\%$ accuracy. A table of these values is included in Appendix A.

Material and thickness data on the actual test specimens are presented in Table 1.

⁸E. Fairstein, "A Nonblocking Double Line Linear Pulse Amplifier," Rev. Sci. Instr. 27(7), 475-82 (1956).

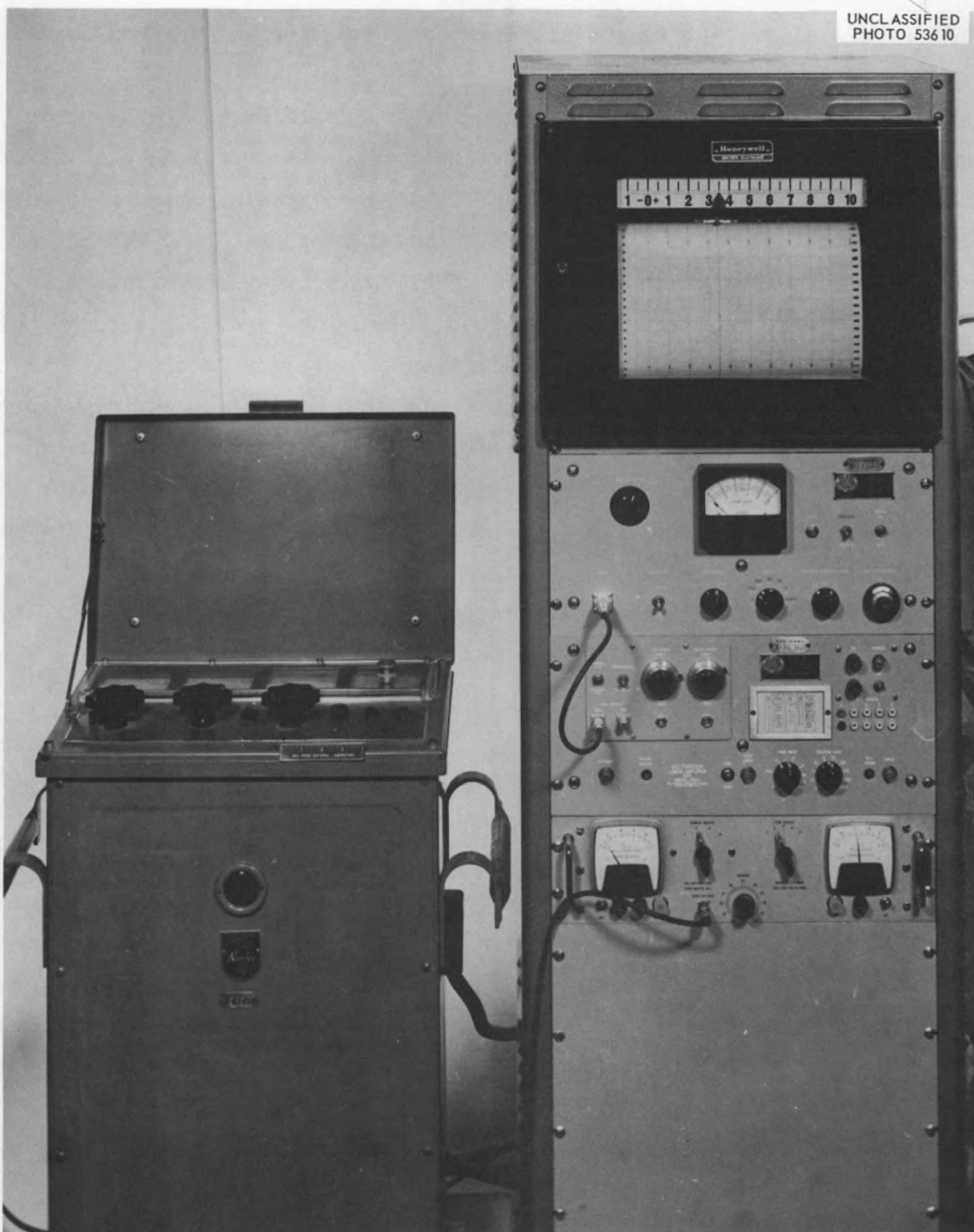


Fig. 2. X-Ray Control Panel, Linear Amplifier, Pulse-Height Analyzer, Linear Count-Rate Meter, and Recorder.

Table 1. Specimen Thicknesses

1100 Aluminum (in.)	Zircaloy-2 ^a (in.)	Type 304 Stainless Steel ^a (in.)	Type 347 Stainless Steel ^a (in.)	Enriched Uranium-Aluminum Alloys		
				7% U (in.)	18% U (in.)	25% U (in.)
0.358	0.110	0.077	0.062	0.256	0.256	0.256
0.312	0.057	0.055	0.039	0.116	0.120	0.120
0.249	0.031	0.020	0.020	0.059	0.030	0.020

^aThe samples not containing uranium were machined and polished to the tabulated thickness with a ± 0.0005 -in. tolerance limit. The uranium-aluminum samples were rolled to the same tolerance.

The density of all samples was determined using the alcohol displacement method. These values are tabulated in Appendix B.

Experimental Procedure

Figure 3 is an illustration of the equipment arrangement and will facilitate the description of the experimental procedure. The x-ray tube head and detector were separated by approximately 12 1/2 ft. This separation was desired to ensure a narrow beam of x rays at the detector without the necessity of pinhole collimation. Photon beams, to be designated narrow, should not be larger than 0.01 steradian.⁹ In this instance, the beam was 0.00014 steradian.

The alignment of the x-ray tube head, collimators, and detector was accomplished with a series of radiographs at each stage of the collimation and, subsequently, at the detector.

Preliminary measurements indicated that there was radiation leakage at the tube head. From a radiographic standpoint, this leakage was negligible. But with the high precision needed and the sensitive detection system used, it was of considerable concern. The problem was solved by completely shielding the x-ray tube from the detector with lead bricks, except for a 3/8-in.-diam port through which the primary beam passed.

⁹G. W. Grodstein, "X-Ray Attenuation Coefficients from 10 kev to 100 Mev," Nat. Bur. Std. (U.S.) Circ. 583, Washington, D. C. (1957).

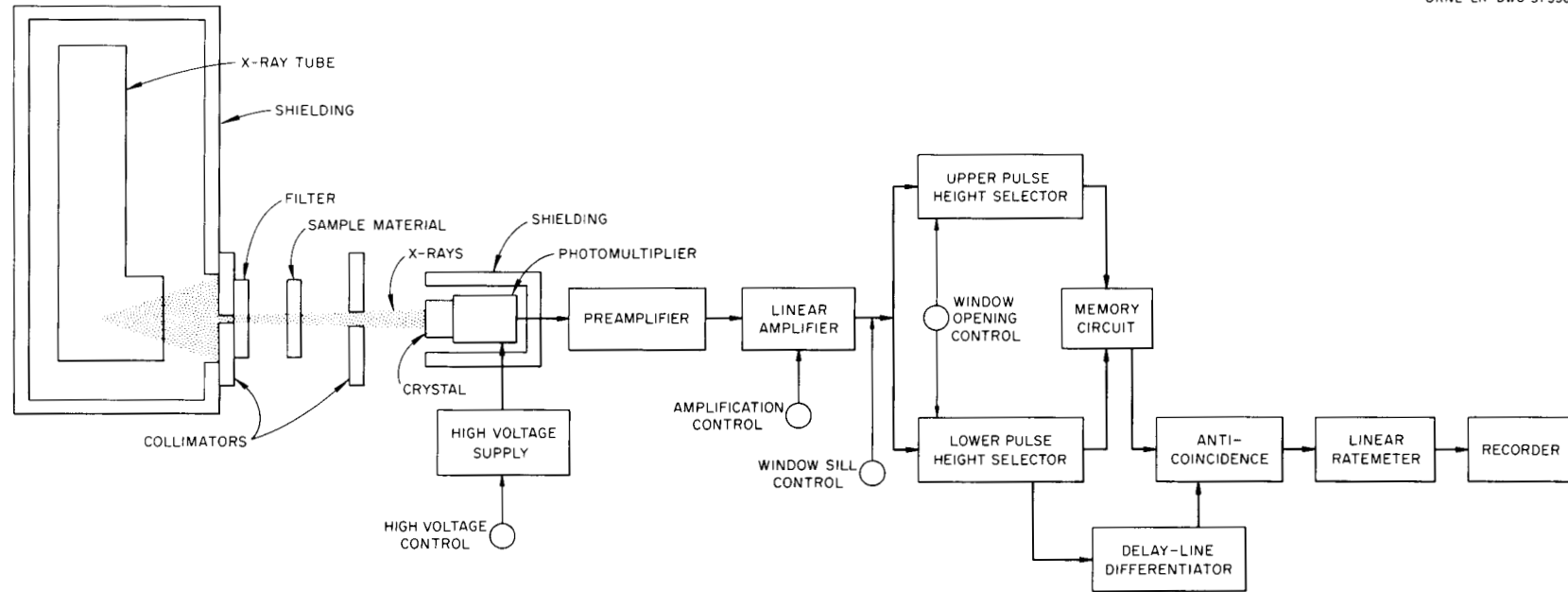


Fig. 3. Block Diagram of X-Ray Equipment Arrangement and Scintillation Spectrometer.

Initial measurements were conducted on an 0.255-in.-thick commercial aluminum sample at 83 kev. The results indicated the necessity for remotely displacing the sample from the x-ray beam. The planned procedure was to monitor the primary x-ray beam intensity for 3 min before the sample was inserted to obtain an average value for the unabsorbed beam. The sample was then inserted and the reduced intensity of the beam monitored for 3 min. Finally, the sample was removed and the unabsorbed beam was again to be measured for 3 min. The first and last measurements should agree, provided no counting rate shift occurs. The center measurement would be an indication of the radiation absorbed. A correlation between the first and last measurements could not be obtained if the x-ray unit was turned off between recordings because of the inherent x-ray tube fluctuations. The problem was eliminated with an assortment of Plexiglas guides and fitted framing designed to allow samples of different thicknesses to be moved remotely in and out of the x-ray beam without removing the power from the unit.

Some x-ray tube instability was noted in the energy range below 40 kev (60 kvp). This instability was a random fluctuation of the tube voltage and amperage. As a result of these fluctuations, the usable range of energies was 40-130 kev.

The calibration of the pulse-height analyzer was accomplished using the gamma radiation of known energies from two isotopes, Sn^{113} and U^{235} . The gain of the linear amplifier was simply adjusted until the gamma peaks were obtained at convenient settings of the energy (E) dial on the amplifier. From these dial readings, the kilo-electron volt per division calibration was obtained. Then, at any dial setting, the kilo-electron volt could be calculated with the product of the kilo-electron volt per division and dial reading. These data provided a linearity check of the system as well. The equipment calibration was performed twice daily, and corrections were made for any calibration change.

The voltage output of the photomultiplier tube has been defined as the pulse height. The height of each pulse from the crystal photomultiplier and amplifier combination is proportional to the amount of incident x-ray energy dissipated by the detector.

These small voltage pulses from the photomultiplier are fed through a preamplifier to a linear amplifier and pulse-height analyzer for shaping and selection between two definite voltage levels. The output from the pulse-height analyzer then goes to a linear count-rate meter and finally to a recorder.

Data Processing

As noted in the experimental procedure, the level of the recorded data was controlled in three ways: (1) there was control of the input voltage to the x-ray tube head, (2) the copper filtration removed much of the softer x rays and sharpened the x-ray spectrum, and (3) the pulse-height analyzer rejected those signals from energies above and below that being monitored. The counting data were recorded at 5-keV increments of effective x-ray energies. Each data period was of 3-min duration. The recorded data were then averaged at 18-sec counting intervals to obtain a mean counting rate. A typical recording with the sample in and out of the x-ray beam is shown in Fig. 4.

Lambert's law was applied to compute the experimental total attenuation coefficients which are listed in Appendix C. This law, as applied to x rays, is

$$\frac{I}{I_0} = e^{-\mu_{\ell}x} \quad (1)$$

where

I_0 = incident photon intensity without the sample in the beam path,

I = photon intensity after the sample has been inserted into the beam path,

x = thickness of the sample, and

μ_{ℓ} = linear attenuation coefficient.¹⁰

The quantity, μ_{ℓ} , is directly dependent on the physical state of the matter traversed by x radiation. A coefficient on a mass basis, which is

¹⁰W. T. Sproull, X-Rays in Practice, McGraw-Hill, New York, 1946.

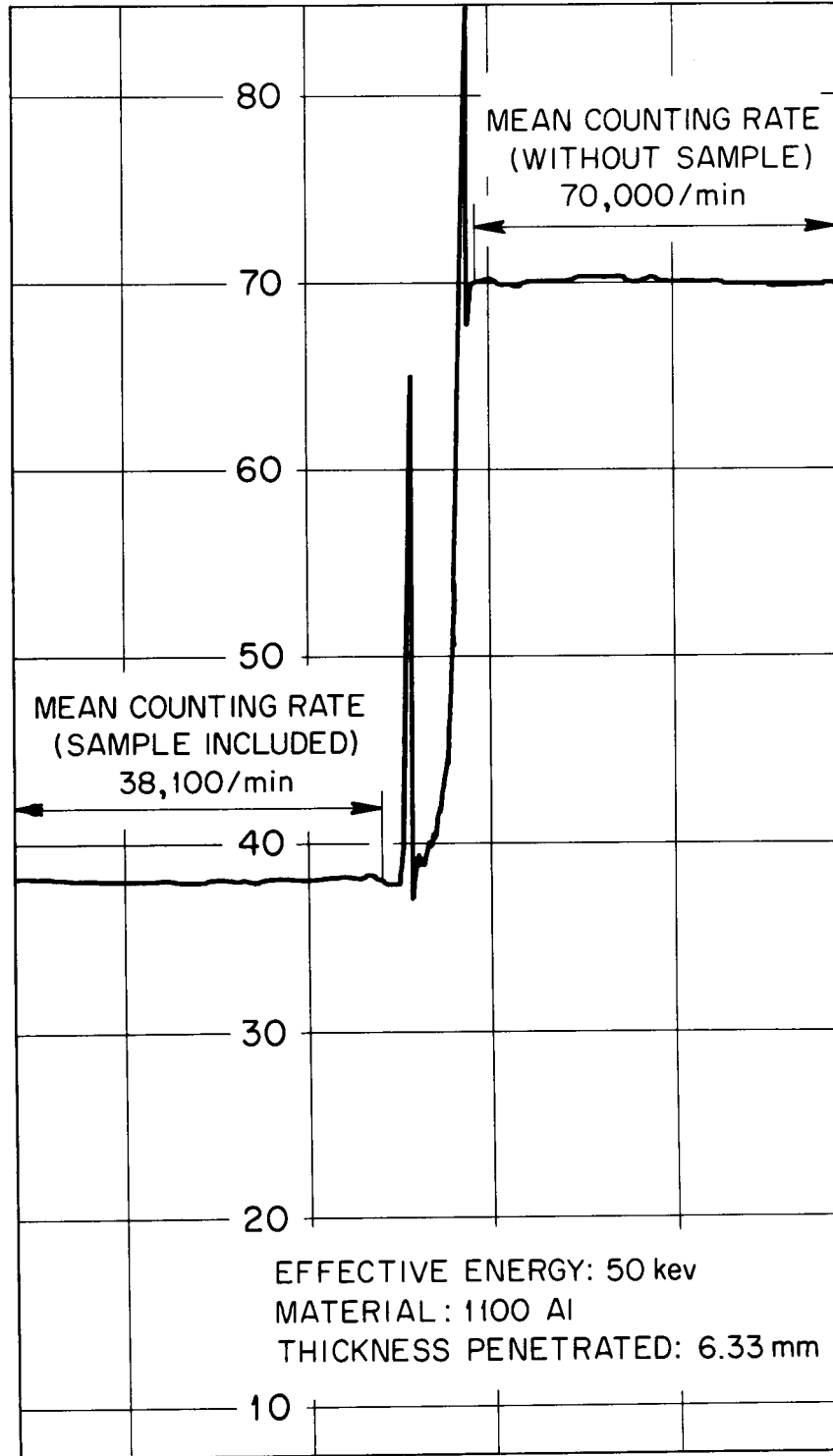
UNCLASSIFIED
ORNL-LR-DWG 60539

Fig. 4. Typical X-Ray Counting with the Sample Materials In and Out of the X-Ray Beam.

independent of the physical state of the absorber, has been more frequently measured and used. The mass attenuation coefficient, μ_m , is the linear attenuation coefficient divided by the density of the absorber.

A final equation of

$$\mu_m = \frac{-\ln \frac{I}{I_0}}{xp} \quad (2)$$

for the experimental determination of the mass attenuation coefficient was found by substitution for μ_l and rearrangement of Lambert's equation.

For a given alloy, the approximation for the total mass absorption coefficient is the summation of the absorbing effects from each of the significant elements. Therefore, for an alloy containing several significant elements in its composition, the mass absorption coefficient at a given energy is

$$\mu_{m_a} = f_1\mu_{m_1} + f_2\mu_{m_2} + f_3\mu_{m_3} + \dots \quad (3)$$

where

μ_{m_a} = mass absorption coefficient for the alloy,

f_1 , f_2 , and f_3 = element weight fractions, and

μ_{m_1} , μ_{m_2} , and μ_{m_3} = element absorption coefficients.¹¹

Theoretical coefficients for each of the materials were determined by the latter equation using the tabulated weight fractions in Appendix A and element attenuation coefficients as listed by Grodstein,¹² Storm,¹³ and White.¹⁴

Representative curves were then computed to an approximate equation of a general hyperbola form by a least-squares fit using a digital computer. These curves and the experimental curves obtained from Lambert's

¹¹R. D. Evans, The Atomic Nucleus, McGraw-Hill, New York, 1955.

¹²G. W. Grodstein, "X-Ray Attenuation Coefficients from 10 kev to 100 Mev," Nat. Bur. Std. (U.S.) Circ. 583, Washington, D. C. (1957).

¹³E. Storm, E. Gilbert, and H. Israel, Gamma Ray Absorption Coefficients for Elements 1 through 100 Derived from the Theoretical Values of The National Bureau of Standards, LA-2237, Los Alamos Scientific Laboratory (1958).

¹⁴G. R. White, "X-Ray Attenuation Coefficients from 10 kev to 100 Mev," Nat. Bur. Std. (U.S.) Rept. 1003, Washington, D. C. (1952).

law are shown in Figs. 5-12. The curves represent the data of the attenuation coefficients only in the comparatively small energy range considered. Therefore, comparisons with functions over an extensive range of energies would not be applicable.

Two possible errors in the experimental determinations should be recognized. These are the shift in the x-ray spectrum when the sample is inserted into the photon beam and the inhomogeneity of the samples. For the first instance, the shift in the spectrum was small since the samples were relatively thin. Attempts were made to distinguish this shift by relocating the x-ray peak after the samples were inserted; however, movement of the peak was too small for the instrument resolution. In the second case, the sample homogeneity proved to be a problem with the uranium-aluminum alloys since uranium tends to segregate. This required the selection of sample specimens based on relative film densities of high-contrast radiographs. However, complete homogeneity cannot be assured even by this method. Figure 13 is a typical radiograph of the uranium-aluminum samples and shows, by the inset circle, the area penetrated by the x radiation.

DISCUSSION ON EXPERIMENTAL AND THEORETICAL DATA

Nonuranium Alloys

A reasonable comparison was observed between the theoretical and experimental results for all the nonuranium alloys as was seen on the respective curves. The deviation in the theoretical and experimental coefficients was small as the energies approached the upper limit of investigation. This was expected since the major change in absorption coefficients for the elements in this program occurs at lower energies.

For alloys that are nearly pure metals, such as Zircaloy-2 and 1100 aluminum, close correlation was also expected. This was the case for Zircaloy-2; however, a small deviation was apparent in the attenuation coefficients for 1100 aluminum at lower energies. The most probable cause of this divergence was the predominant, incoherent scattering interaction which occurs in the elements of lower atomic number.

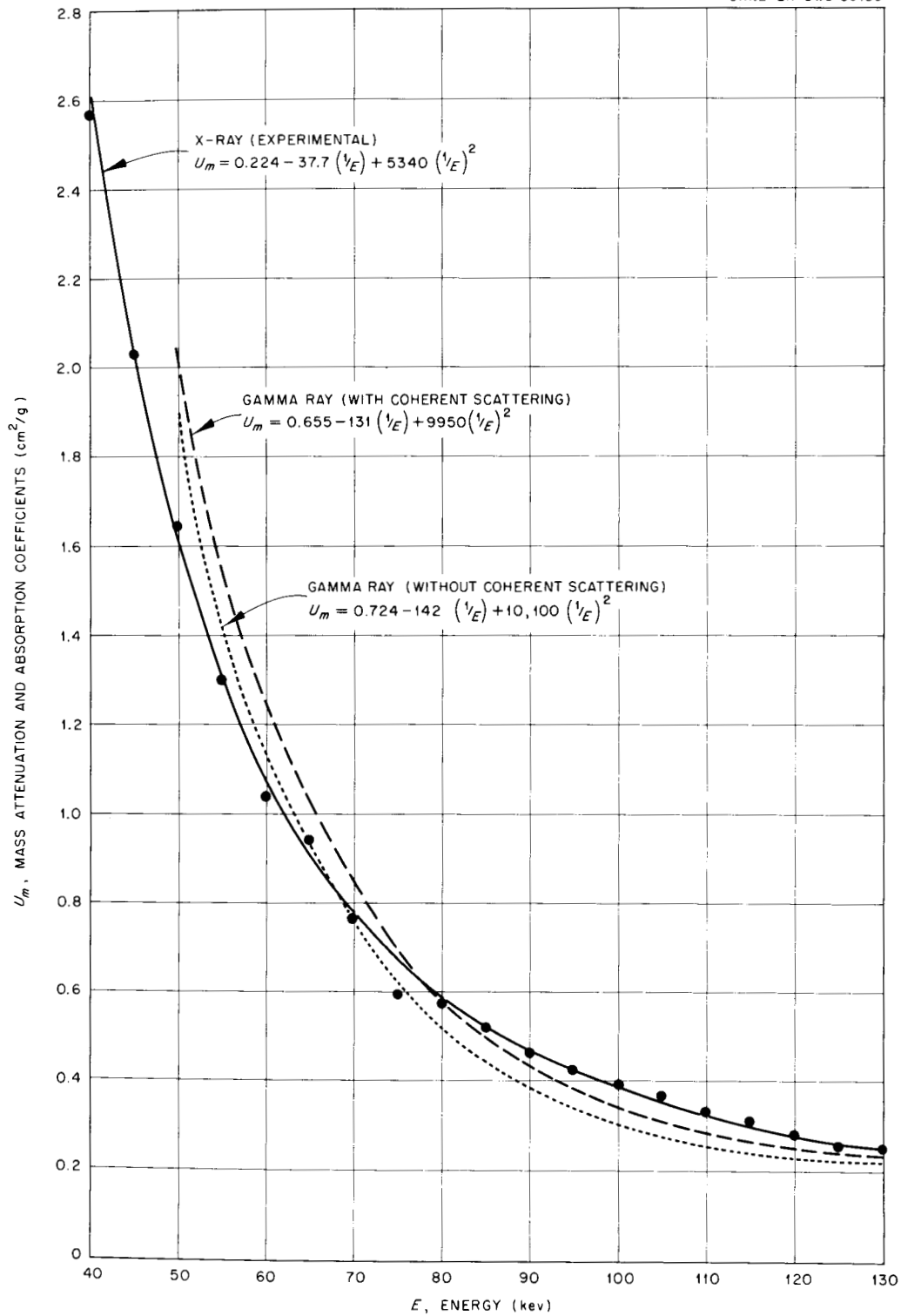


Fig. 5. Effective X-Ray Attenuation Coefficients and Calculated Gamma Ray Absorption Coefficients for Type 347 Stainless Steel.

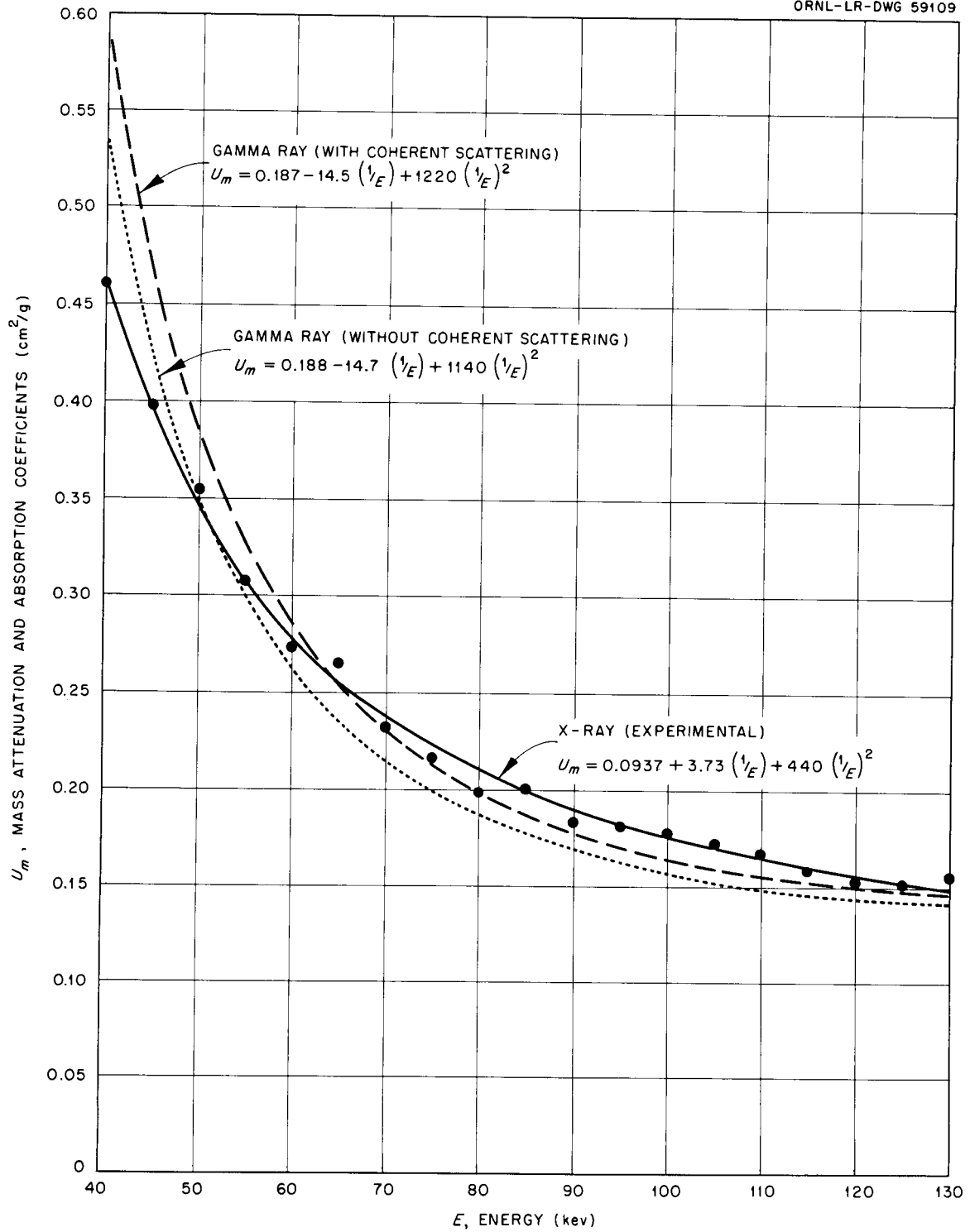


Fig. 6. Effective X-Ray Attenuation Coefficients and Calculated Gamma Ray Absorption Coefficients for 1100 Aluminum.

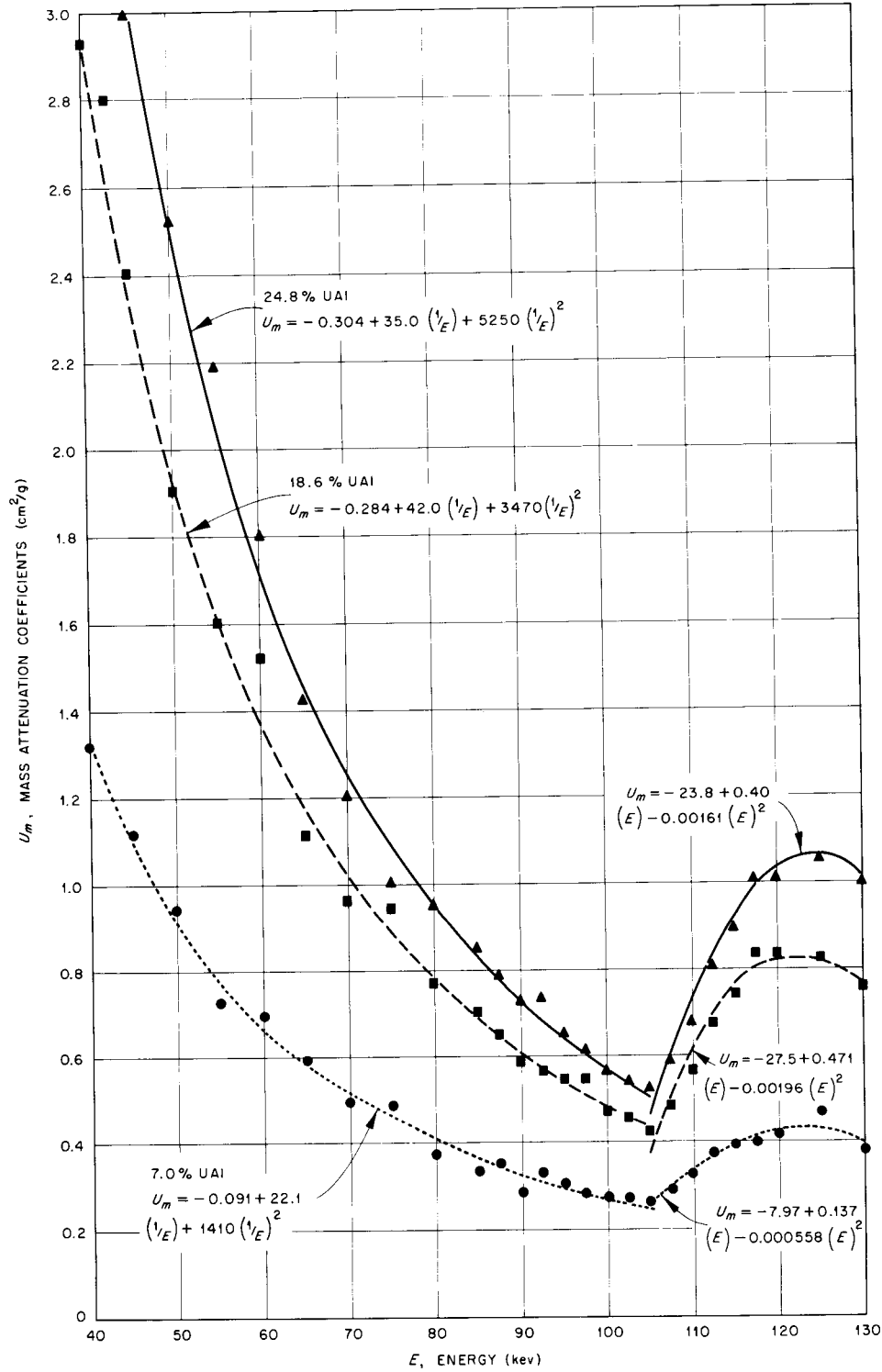
UNCLASSIFIED
ORNL-LR-DWG 59110

Fig. 7. Effective X-Ray Attenuation Coefficients for 24.8, 18.6, and 7 wt % U-Al.

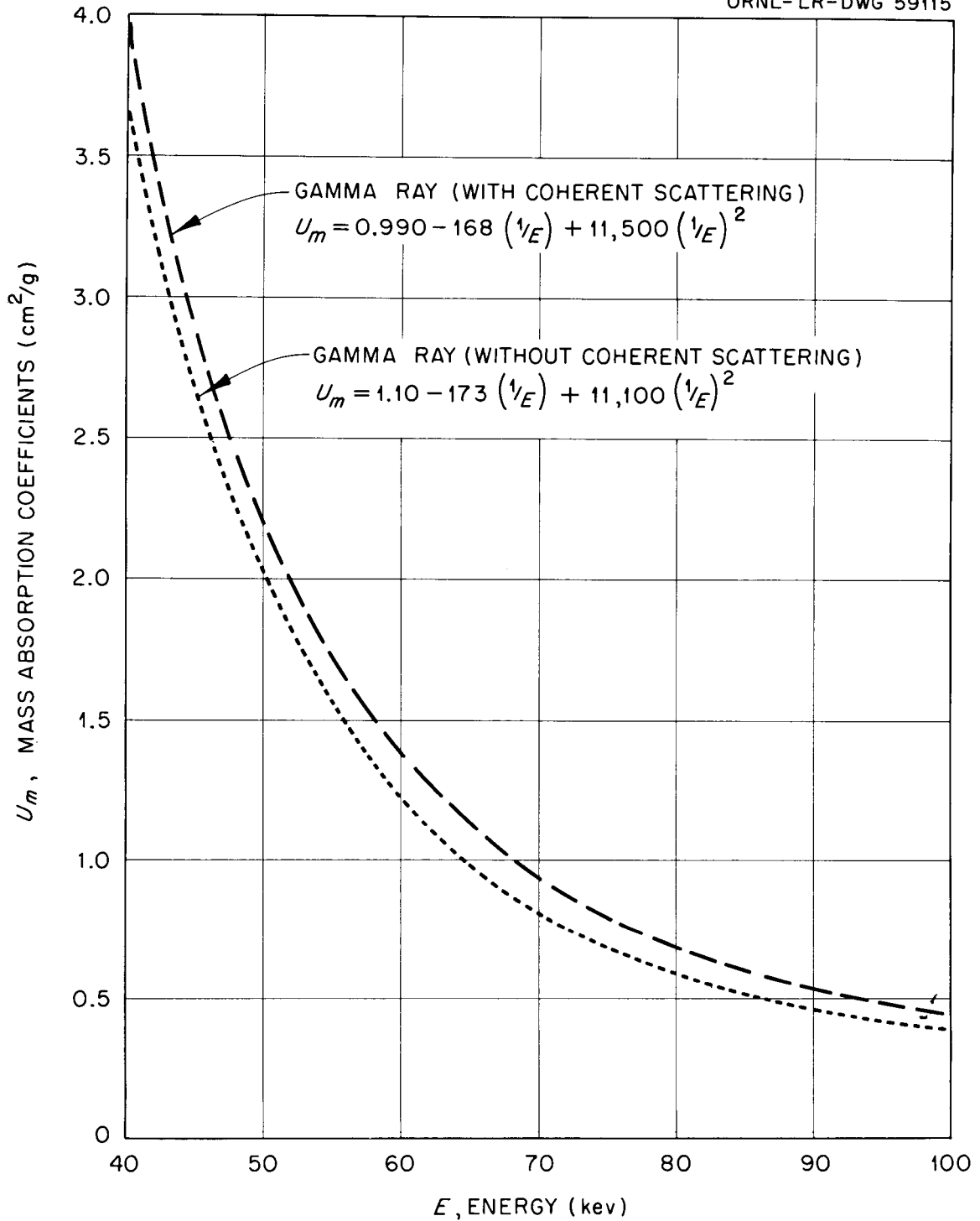
UNCLASSIFIED
ORNL-LR-DWG 59115

Fig. 8. Calculated Gamma Ray Absorption Coefficients for 24.8 wt % U-Al.

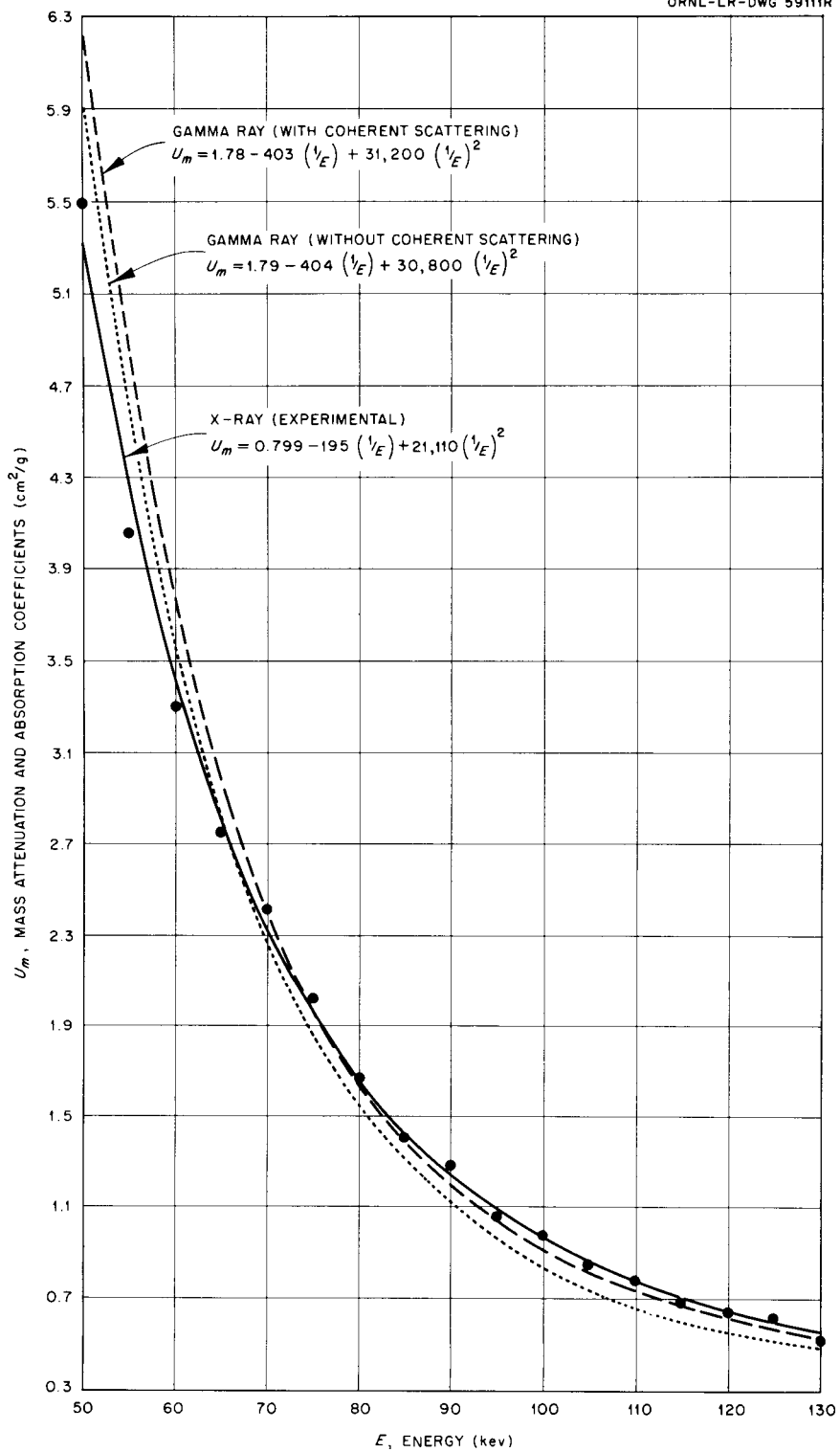
UNCLASSIFIED
ORNL-LR-DWG 59111R

Fig. 9. Effective X-Ray Attenuation Coefficients and Calculated Gamma Ray Absorption Coefficients for Zircaloy-2.

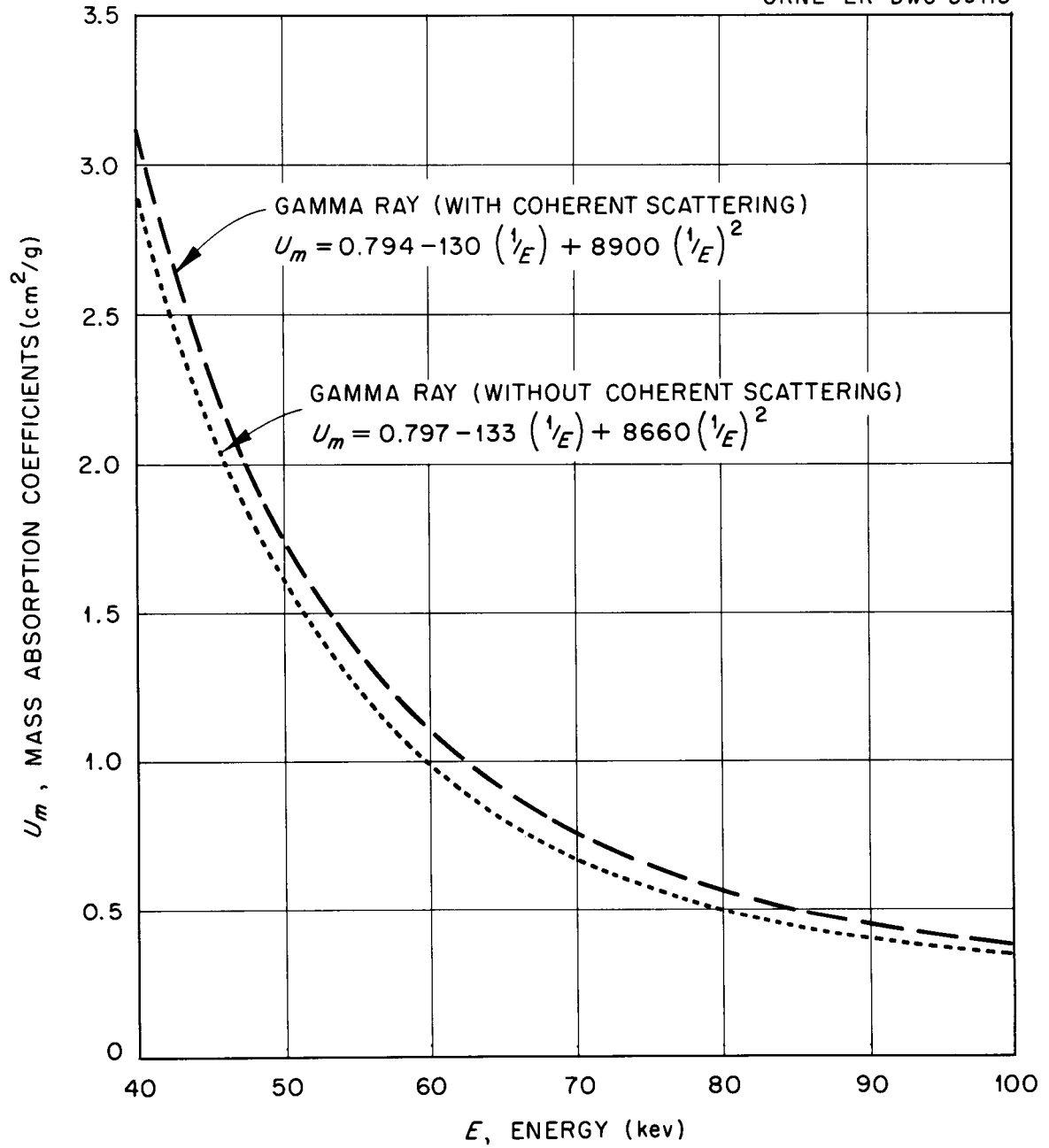
UNCLASSIFIED
ORNL-LR-DWG 59113

Fig. 10. Calculated Gamma Ray Absorption Coefficients for 18.6 wt % U-Al.

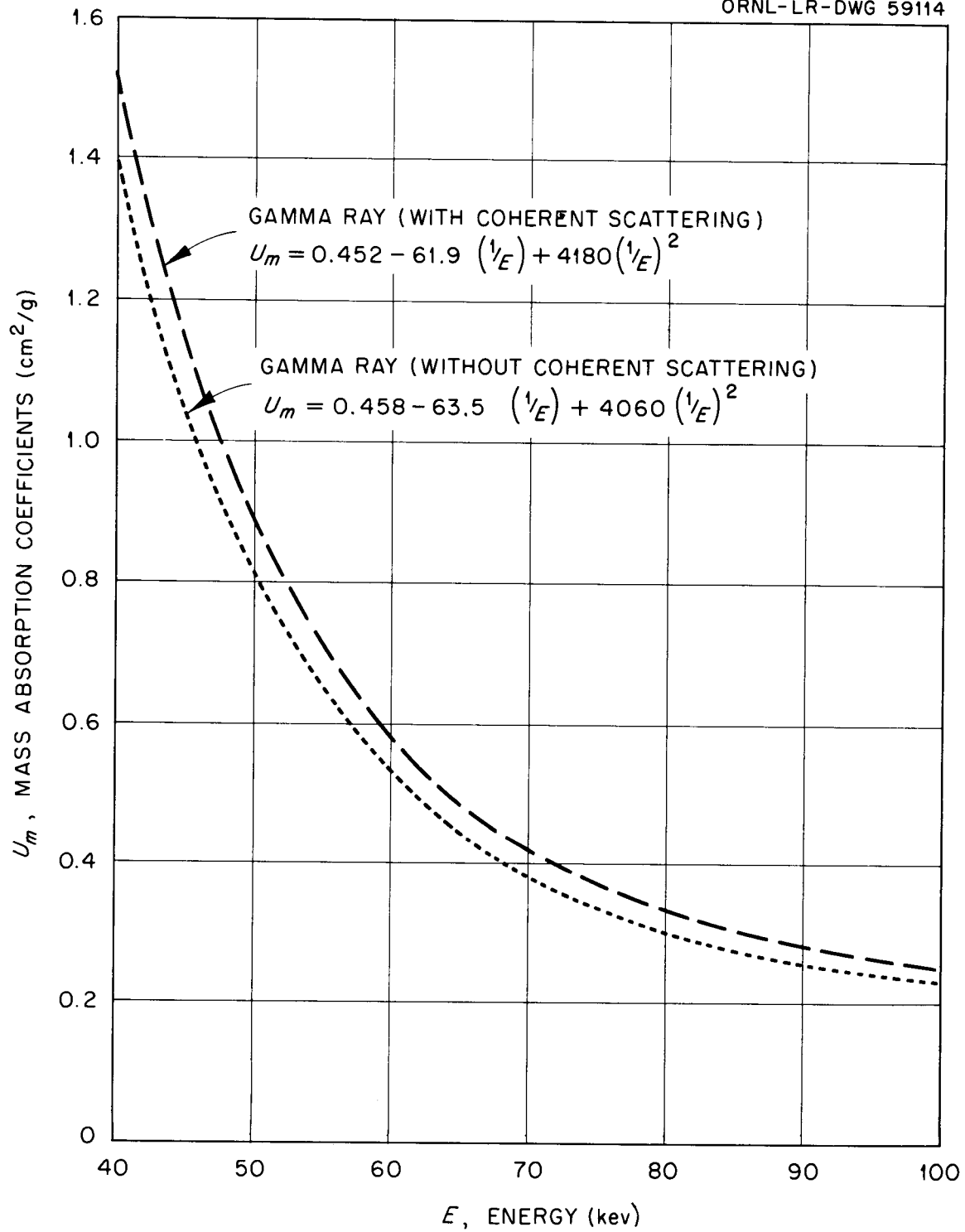
UNCLASSIFIED
ORNL-LR-DWG 59114

Fig. 11. Calculated Gamma Ray Absorption Coefficients for 7 wt % U-Al.

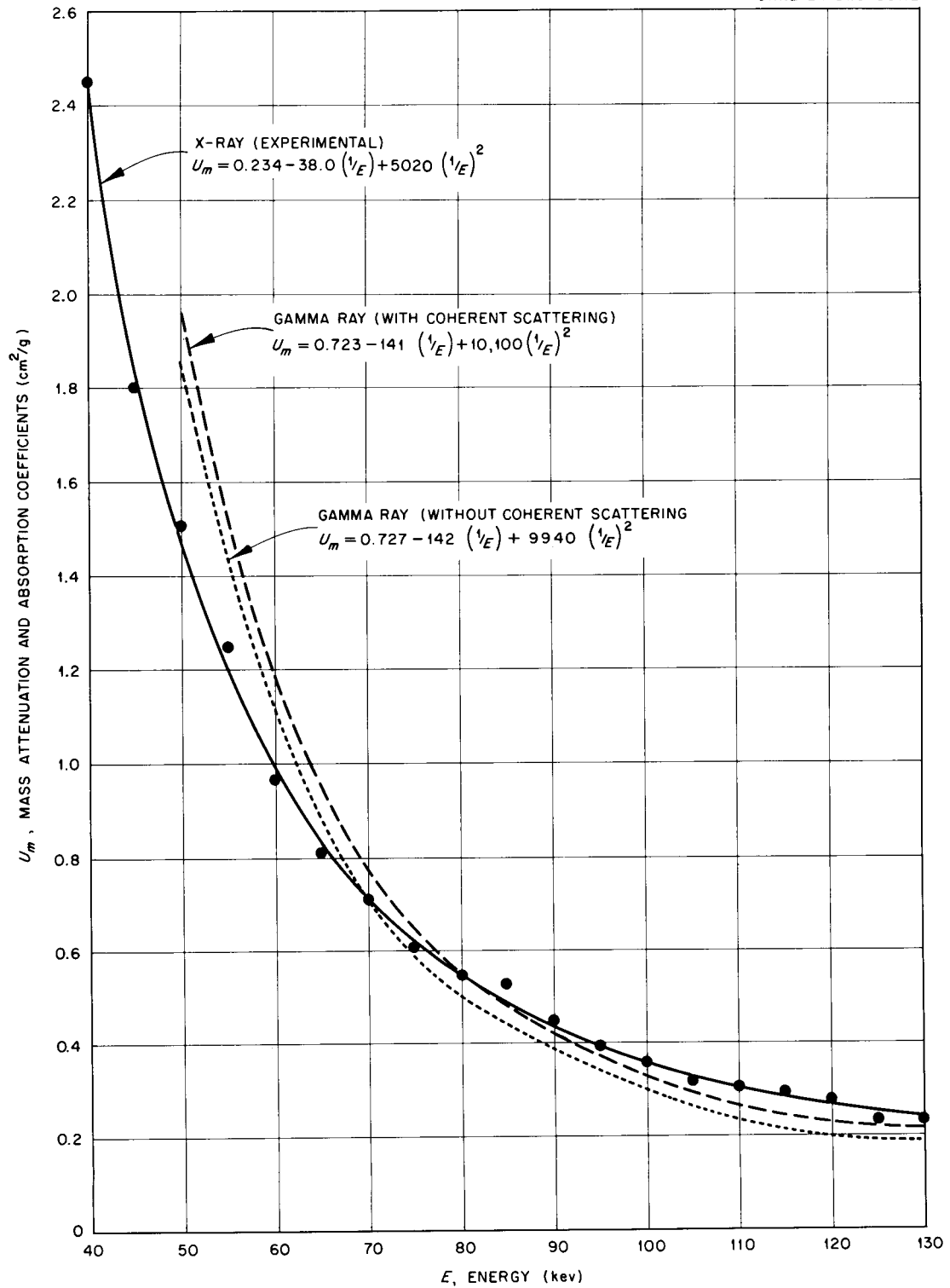
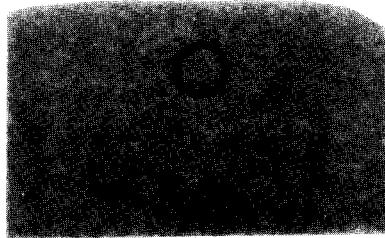
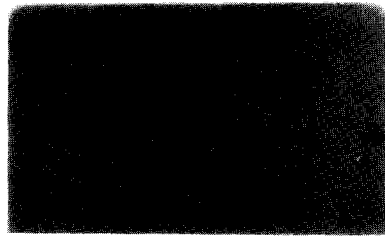


Fig. 12. Effective X-Ray Attenuation Coefficients and Calculated Gamma Ray Absorption Coefficients for Type 304 Stainless Steel.

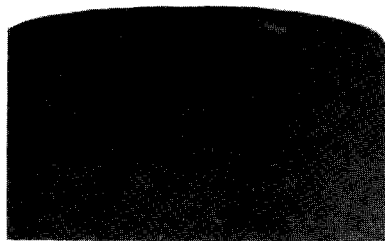
UNCLASSIFIED
PHOTO 53579



248 UAL
120 MILS



70 UAL
250 MILS



186 UAL
120 MILS

Fig. 13. Typical Radiographs of Samples.

The results on stainless steel indicate good correlation considering the number of significant elements in these materials. The energy range of 70-130 kev shows the minimum variation.

Uranium Alloys

A large, consistent deviation was noted in the uranium-aluminum coefficients. The aluminum used in this alloy has high purity and is similar to 1100 aluminum. Since close agreement was apparent in the aluminum specimens which have a very small absorption coefficient compared to uranium, the major source of this deviation was attributed to the element uranium. A large deviation in the theoretical and experimental lower energy absorption coefficients for uranium has been noted also by R. T. McGinnies¹⁵ and R. E. Connally.¹⁶

The only absorption edge encountered in the range of energies in this study was associated with uranium. This absorption edge occurred between 105-130 kev. Despite the fact that considerable efforts sharpened the x-ray beam spectrum and reduced its polychromatic character, there was a spread in the absorption edge since the x rays examined only approached a homogeneous wavelength.

Uranium was also the only element having a sufficient fluorescence energy to be of possible concern in this x-ray energy range. However, the presence of any fluorescence intensity was not apparent. It is believed the intensity of the characteristic x rays of uranium was so small in comparison to the x-ray beam that it had negligible effect in reinforcing the primary beam.

¹⁵R. T. McGinnies, "X-Ray Attenuation Coefficients from 10 kev to 100 Mev," Nat. Bur. Std. (U.S.) Supplement to Circ. 583, Washington, D. C. (1959).

¹⁶R. E. Connally, U. L. Upson, and P. E. Brown, Uranium Analysis by Gamma Absorptiometry, HW-54438, Hanford Atomic Products Operation (1958).

CONCLUSIONS

The experimental results for these alloys provide useful curves that may be used with reliability in measurements of homogeneity, determination of density, or gaging thicknesses. These curves can be readily reproduced provided the counting geometry employed is similar to the one described in this program.

Since the absorption coefficients computed by G. R. White¹⁷ on the element uranium are apparently in error for the lower energies and data of E. Storm et al.¹⁸ were dependent on this element being correct, the investigators recommend further attenuation studies in the lower energies for uranium and the elements with atomic numbers in the proximity of uranium.

The authors recommend further investigations on alloys using a narrow x-ray beam with the sample located nearer the detector. This would increase the accuracy of the overall measurement of homogeneity since a greater volume of penetrated material would be available for chemical analysis. An investigation of this type would require extremely close dimensional tolerance on the specimens.

ACKNOWLEDGMENTS

The authors are most grateful to Nancy M. Dismuke (deceased) for her help in the computer programming and to W. C. Colwell for his assistance in the line drawings. The authors would particularly like to express appreciation to R. W. McClung and W. J. Mason whose assistance, guidance, and helpful suggestions greatly aided the success of this program.

¹⁷G. R. White, "X-Ray Attenuation Coefficients from 10 kev to 100 Mev," Nat. Bur. Std. (U.S.) Rept. 1003, Washington, D. C. (1952).

¹⁸E. Storm, E. Gilbert, and H. Israel, Gamma Ray Absorption Coefficients for Elements 1 through 100 Derived from the Theoretical Values of the National Bureau of Standards, LA-2237, Los Alamos Scientific Laboratory (1958).

APPENDIX A

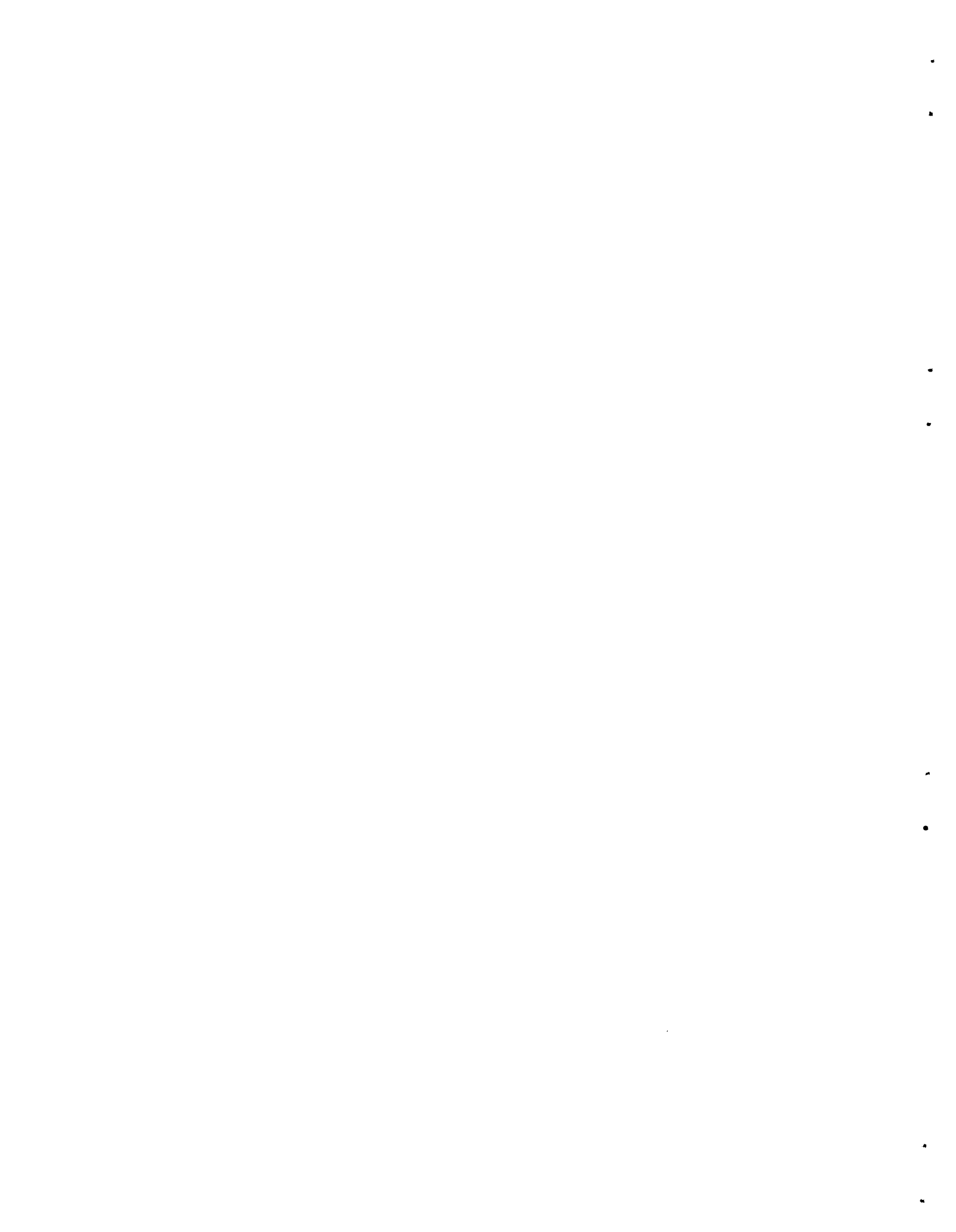


Table 2. Chemical Analysis in Weight Percent for Each Test Material

	Si	Fe	Cu	Zn	Al	Mn	Cr	Ni	C	Nb	Zr	Sn	U
Type 304 Stainless Steel	0.5	71.4	a	a	a	1.0	17.3	9.8	a	a	a	a	a
Type 347 Stainless Steel	0.4	69.3	a	a	a	1.2	17.9	10.4	a	0.8	a	a	a
Zircaloy-2	a	a	a	a	a	a	a	a	a	a	98.6	1.4	a
1100 Aluminum	0.1	0.6	0.2	0.1	99.0	a	a	a	a	a	a	a	a
Uranium-Aluminum	a	a	a	a	75.2	a	a	a	a	a	a	a	24.8
Uranium-Aluminum	a	a	a	a	81.4	a	a	a	a	a	a	a	18.6
Uranium-Aluminum	a	a	a	a	93.0	a	a	a	a	a	a	a	7.0

^aLess than 0.1 wt % or negligible.

•

•

•

•

•

•

•

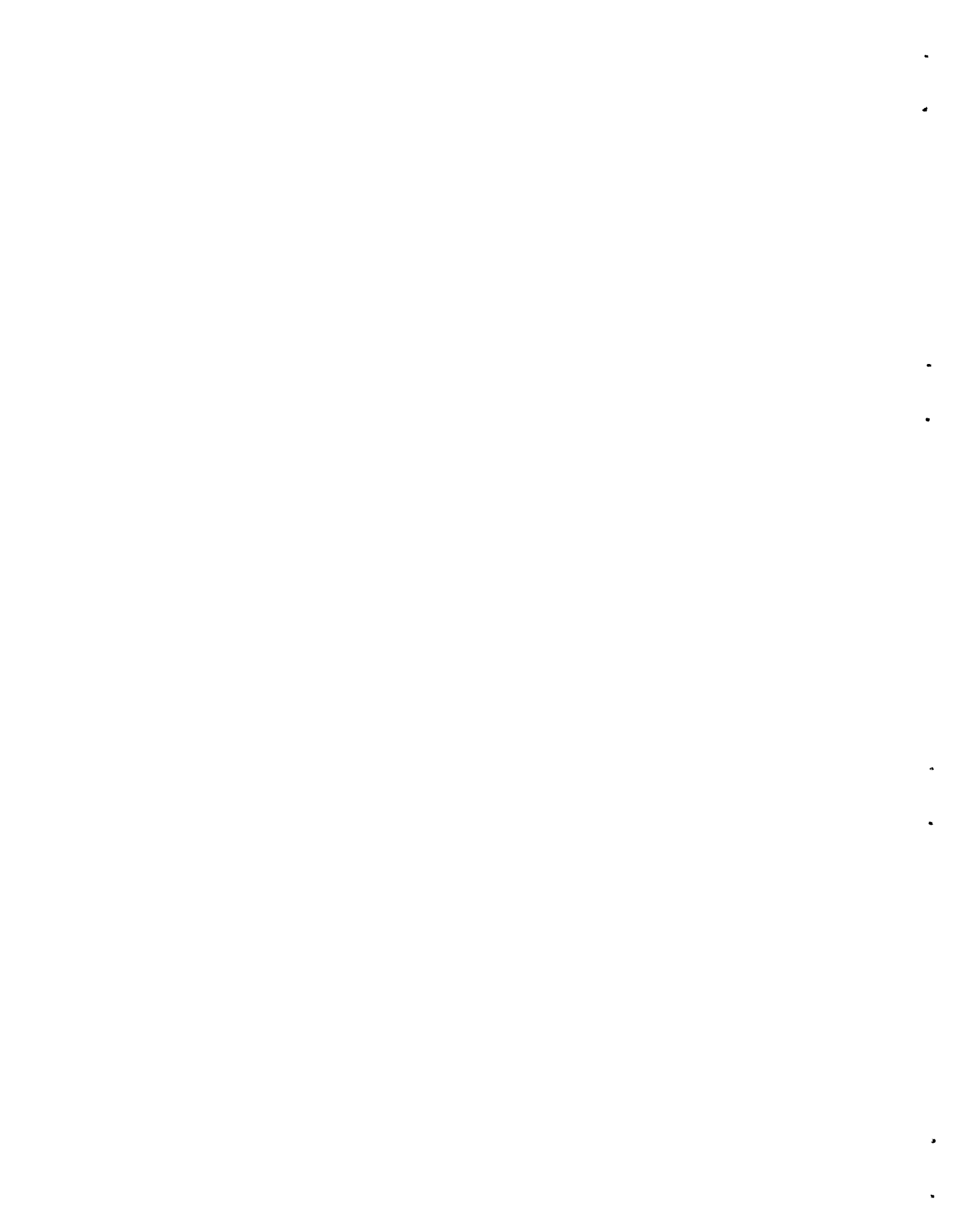
•

APPENDIX B



Table 3. Density Measurements on All Samples

Specimen Material	Specimen Thickness (mm)	Weight in Air (g)	Weight in Alcohol (g)	Alcohol Temperature (°C)	Alcohol Density (g/cm ³)	Difference in Weight (g)	Specimen Volume (cm ³)	Specimen Density (g/cm ³)
1100 Aluminum	6.33	55.1109	39.1777	25.8	0.78454	15.9332	20.3090	2.7136
1100 Aluminum	7.94	69.1902	49.1974	26.3	0.78410	19.9928	25.4978	2.7136
1100 Aluminum	9.11	79.2038	56.3182	26.2	0.78420	22.8856	29.1834	2.7140
Type 304 Stainless Steel	0.505	12.8038	11.5304	26.0	0.78438	1.2734	1.6234	7.8870
Type 304 Stainless Steel	1.40	35.9487	32.3956	28.4	0.78232	3.5531	4.5418	7.9151
Type 304 Stainless Steel	1.96	50.0363	45.0756	26.0	0.78438	4.9607	6.3244	7.9116
Type 347 Stainless Steel	0.510	12.9652	11.6783	26.0	0.78438	1.2869	1.6407	7.9022
Type 347 Stainless Steel	1.00	25.6359	23.0959	26.0	0.78438	2.5400	3.2382	7.9167
Type 347 Stainless Steel	1.57	40.0124	36.0508	26.0	0.78438	3.9616	5.0506	7.9223
Zircaloy-2	0.800	17.3670	15.2926	28.6	0.78216	2.0744	2.6521	6.5484
Zircaloy-2	1.44	30.2213	26.6003	26.0	0.78438	3.6210	4.6164	6.5465
Zircaloy-2	2.79	58.4314	51.4296	25.9	0.78446	7.0018	8.9256	6.5465
24.8 wt % U-Al	0.508	2.7340	2.0918	25.3	0.78496	0.6422	0.8181	3.3419
24.8 wt % U-Al	3.04	16.1341	12.3630	25.3	0.78496	3.7711	4.8042	3.3583
24.8 wt % U-Al	6.52	34.7521	26.6415	25.3	0.78496	8.1106	10.3325	3.3634
18.6 wt % U-Al	0.754	3.8687	2.9086	25.4	0.78488	0.9601	1.2232	3.1628
18.6 wt % U-Al	3.05	14.9911	11.2975	25.4	0.78488	3.6936	4.7059	3.1856
18.6 wt % U-Al	6.53	32.9381	24.7769	25.3	0.78496	8.1612	10.3970	3.1680
7.0 wt % U-Al	1.51	7.0246	5.0953	25.2	0.78502	1.9293	2.4576	2.8583
7.0 wt % U-Al	2.97	13.1536	9.5442	25.2	0.78502	3.6094	4.5978	2.8609
7.0 wt % U-Al	6.51	29.0267	21.0580	25.2	0.78502	7.9687	10.1510	2.8595



APPENDIX C



APPENDIX C

A sample determination of the experimental mass attenuation coefficient of type 304 stainless steel is given as a guide to the experimenter.

As noted in Table 4 for type 304 stainless steel at any energy of 40 kev,

Counting rate I = 24,200,

Counting rate I₀ = 64,000,

Thickness = 0.505 mm, and

Density = 7.89 g/cc.

Substituting these values in Eq. 2 of the text,

$$\mu_m = \frac{-\ln \frac{I}{I_0}}{xp} = \frac{-\ln \frac{24.2}{64.0}}{(0.0505 \text{ cm})(7.89 \text{ g/cc})}$$

$$\mu_m = 2.45 \text{ cm}^2/\text{g}$$

Table 4. Type 304 Stainless Steel Data

Effective Energy (kev)	X-ray Control (kvcp)	X-ray Control (ma)	Copper Filtration (mm)	Counting Rate I With Sample (min ⁻¹)	Counting Rate I ₀ Without Sample (min ⁻¹)
40	58	10.3	3.18	24,200	64,000
45	64	18.7	4.76	16,900	34,700
50	66	14.3	4.76	48,400	88,000
55	73	14.3	6.35	50,800	83,500
60	79	15.1	7.94	59,000	86,700
65	83	14.3	9.52	51,800	71,600
70	88	12.3	11.1	70,200	93,200
75	92	11.0	12.7	75,600	96,300
80	96	10.8	14.3	45,400	82,800
85	103	14.8	17.5	41,500	74,300
90	106	13.9	20.6	24,200	39,700
95	112	8.7	17.5	25,200	39,400
100	118	8.5	23.8	51,400	67,800
105	121	9.8	22.2	32,800	46,400
110	129	13.0	27.0	28,600	45,700
115	134	7.2	28.6	29,500	46,100
120	138	9.8	27.0	46,500	63,300
125	147	7.6	34.9	37,200	53,400
130	151	8.0	36.5	37,700	54,000

Table 5. Additional Data and Attenuation Coefficients
for Type 304 Stainless Steel

Effective Energy (kev)	Sample Thickness (mm)	Sample Density (g/cm ³)	μ_l Linear Attenuation Coefficient (cm ⁻¹)	μ_m Mass Attenuation Coefficient (cm ² /g)
40	0.505	7.89	19.3	2.45
45	0.505	7.89	14.2	1.80
50	0.505	7.89	11.9	1.51
55	0.505	7.89	9.85	1.25
60	0.505	7.89	7.64	0.968
65	0.505	7.89	6.40	0.811
70	0.505	7.89	5.62	0.712
75	0.505	7.89	4.79	0.607
80	1.40	7.91	4.30	0.544
85	1.40	7.91	4.17	0.527
90	1.40	7.91	3.55	0.449
95	1.40	7.91	3.21	0.406
100	1.40	7.91	2.78	0.352
105	1.40	7.91	2.49	0.315
110	1.96	7.91	2.40	0.303
115	1.96	7.91	2.28	0.288
120	1.40	7.91	2.21	0.279
125	1.96	7.91	1.85	0.234
130	1.96	7.91	1.83	0.231

Table 6. Type 347 Stainless Steel Data

Effective Energy (kev)	X-Ray Control (kvcp)	X-Ray Control (ma)	Copper Filtration (mm)	Counting Rate I With Sample (min^{-1})	Counting Rate I_0 Without Sample (min^{-1})
40	57	13.1	3.18	15,000	42,400
45	60	10.2	3.43	38,800	90,200
50	66	10.1	4.76	37,900	73,500
55	71	10.4	6.35	29,000	49,100
60	76	11.4	7.94	38,400	58,300
65	81	12.5	9.52	37,000	54,100
70	86	12.0	11.1	46,100	62,900
75	91	12.0	12.7	57,200	72,700
80	96	9.5	14.3	46,300	73,200
85	101	9.9	17.5	45,600	56,200
90	103	11.0	19.0	33,900	49,100
95	108	11.5	20.6	41,200	57,600
100	113	9.2	17.5	39,200	53,600
105	118	9.6	20.6	31,500	42,200
110	127	10.0	25.4	27,100	40,600
115	130	10.1	27.0	33,500	43,000
120	136	9.2	30.2	29,500	41,800
125	141	10.1	31.8	46,600	64,000
130	146	10.3	34.9	41,100	56,000

Table 7. Additional Data and Attenuation Coefficients
for Type 347 Stainless Steel

Effective Energy (kev)	Sample Thickness (mm)	Sample Density (g/cm ³)	μ_l Linear Attenuation Coefficient (cm ⁻¹)	μ_m Mass Attenuation Coefficient (cm ² /g)
40	0.510	7.90	20.3	2.57
45	0.510	7.90	16.5	2.09
50	0.510	7.90	13.0	1.65
55	0.510	7.90	10.3	1.30
60	0.510	7.90	8.18	1.04
65	0.510	7.90	7.45	0.943
70	0.510	7.90	6.10	0.772
75	0.510	7.90	4.72	0.597
80	1.00	7.92	4.57	0.577
85	0.510	7.90	4.14	0.524
90	1.00	7.92	3.71	0.468
95	1.00	7.92	3.35	0.423
100	1.00	7.92	3.13	0.395
105	1.00	7.92	2.93	0.370
110	1.57	7.92	2.56	0.323
115	1.00	7.92	2.50	0.316
120	1.57	7.92	2.24	0.283
125	1.57	7.92	2.02	0.255
130	1.57	7.92	1.98	0.250

Table 8. Zircaloy-2 Data

Effective Energy (kev)	X-Ray Control (kvcp)	X-Ray Control (ma)	Copper Filtration (mm)	Counting Rate I With Sample (min^{-1})	Counting Rate I ₀ Without Sample (min^{-1})
50	66	18.7	4.76	5,200	92,400
55	73	10.2	6.35	10,000	84,000
60	78	11.2	7.94	12,900	73,000
65	82	12.0	9.52	16,700	70,500
70	87	12.7	11.1	19,600	67,600
75	91	13.0	12.7	25,800	74,600
80	98	15.8	15.9	10,000	50,000
85	104	14.9	12.7	15,700	59,460
90	107	15.9	14.3	16,970	57,000
95	112	14.9	17.5	18,800	51,100
100	118	13.0	20.6	18,000	45,300
105	123	11.9	23.8	15,900	35,400
110	127	11.8	25.4	23,800	49,600
115	132	11.0	28.6	22,700	43,100
120	139	8.2	30.2	34,400	63,000
125	142	9.0	33.3	12,900	38,400
130	148	9.0	36.5	15,800	40,600

Table 9. Additional Data and Attenuation Coefficients
for Zircaloy-2

Effective Energy (kev)	Sample Thickness (mm)	Sample Density (g/cm ³)	μ_L Linear Attenuation Coefficient (cm ⁻¹)	μ_m Mass Attenuation Coefficient (cm ² /g)
50	0.80	6.55	36.0	5.50
55	0.80	6.55	26.6	4.06
60	0.80	6.55	21.6	3.30
65	0.80	6.55	18.0	2.75
70	0.80	6.55	15.5	2.37
75	0.80	6.55	13.3	2.03
80	1.44	6.55	11.2	1.71
85	1.44	6.55	9.25	1.41
90	1.44	6.55	8.41	1.28
95	1.44	6.55	6.96	1.06
100	1.44	6.55	6.42	0.980
105	1.44	6.55	5.56	0.849
110	1.44	6.55	5.10	0.779
115	1.44	6.55	4.45	0.679
120	1.44	6.55	4.20	0.641
125	2.79	6.55	3.91	0.597
130	2.79	6.55	3.37	0.514

Table 10. Data for 1100 Aluminum

Effective Energy (kev)	X-Ray Control (kvcp)	X-Ray Control (ma)	Copper Filtration (mm)	Counting Rate I With Sample (min^{-1})	Counting Rate I_0 Without Sample (min^{-1})
40	58	10.5	3.18	21,400	46,700
45	60	10.5	3.43	48,400	95,900
50	66	11.4	4.76	38,100	70,000
55	70	12.0	6.35	19,900	37,100
60	77	11.5	7.94	32,200	51,500
65	81	14.0	9.52	15,700	43,100
70	86	14.3	11.1	26,400	43,600
75	92	14.7	12.7	49,900	79,500
80	96	15.6	14.3	61,600	92,600
85	101	12.6	17.5	40,700	63,900
90	105	9.5	12.7	16,500	26,000
95	110	6.7	14.3	46,600	72,800
100	113	7.9	15.9	60,700	94,400
105	118	9.5	19.0	48,500	74,100
110	123	10.0	22.2	54,100	82,900
115	129	9.8	25.4	42,100	62,200
120	135	9.5	28.6	47,300	68,800
125	142	9.0	31.8	40,500	58,900
130	149	6.2	34.9	34,200	50,300

Table 11. Additional Data and Attenuation Coefficients
for 1100 Aluminum

Effective Energy (kev)	Sample Thickness (mm)	Sample Density (g/cm ³)	μ_{ρ} Linear Attenuation Coefficient (cm ⁻¹)	μ_m Mass Attenuation Coefficient (cm ² /g)
40	6.33	2.71	1.23	0.454
45	6.33	2.71	1.08	0.398
50	6.33	2.71	0.962	0.355
55	6.33	2.71	0.836	0.308
60	6.33	2.71	0.739	0.273
65	7.94	2.71	0.722	0.266
70	7.94	2.71	0.628	0.232
75	7.94	2.71	0.586	0.216
80	7.94	2.71	0.514	0.198
85	7.94	2.71	0.568	0.201
90	9.11	2.71	0.495	0.183
95	9.11	2.71	0.490	0.181
100	9.11	2.71	0.482	0.178
105	9.11	2.71	0.466	0.172
110	9.11	2.71	0.470	0.173
115	9.11	2.71	0.428	0.158
120	9.11	2.71	0.412	0.152
125	9.11	2.71	0.410	0.151
130	9.11	2.71	0.422	0.156

Table 12. Data for 7 wt % U-Al

Effective Energy (kev)	X-Ray Control (kvcp)	X-Ray Control (ma)	Copper Filtration (mm)	Counting Rate I With Sample (min^{-1})	Counting Rate I_0 Without Sample (min^{-1})
40.0	56	10.0	2.86	41,200	72,800
45.0	62	10.0	3.69	49,300	80,000
50.0	66	5.0	4.45	58,200	87,600
55.0	70	5.0	5.52	58,400	80,000
60.0	73	10.0	6.35	67,600	92,600
65.0	83	12.0	9.21	64,400	83,000
70.0	88	12.0	10.8	64,800	80,300
75.0	94	12.5	14.0	64,100	79,000
80.0	98	13.0	15.1	60,000	82,500
85.0	103	12.7	17.5	59,000	78,700
87.5	106	12.5	18.8	48,200	65,100
90.0	110	13.0	20.6	62,900	78,600
92.5	112	12.5	21.6	50,000	66,300
95.0	115	14.0	23.0	55,300	71,600
97.5	118	11.5	24.3	48,700	62,000
100.0	122	10.0	20.3	59,900	75,500
102.5	123	10.5	21.1	64,200	81,000
105.0	126	10.0	22.2	51,600	84,000
107.5	131	10.5	25.4	41,300	71,500
110.0	134	10.5	27.0	39,100	72,000
112.5	137	10.0	28.6	34,900	69,900
115.0	140	12.0	30.2	31,800	65,900
117.5	143	10.0	31.8	28,700	62,200
120.0	149	11.0	33.3	41,300	89,300
125.0	153	10.5	34.9	39,900	84,300
130.0	156	11.0	36.5	43,600	87,900

Table 13. Additional Data and Attenuation Coefficients
for 7 wt % U-Al

Effective Energy (kev)	Sample Thickness (mm)	Sample Density (g/cm ³)	μ_l Linear Attenuation Coefficient (cm ⁻¹)	μ_m Mass Attenuation Coefficient (cm ² /g)
40.0	1.51	2.86	3.77	1.32
45.0	1.51	2.86	3.21	1.12
50.0	1.51	2.86	2.70	0.944
55.0	1.51	2.86	2.08	0.727
60.0	1.51	2.86	1.99	0.696
65.0	1.51	2.86	1.68	0.587
70.0	1.51	2.86	1.43	0.496
75.0	1.51	2.86	1.39	0.486
80.0	2.97	2.86	1.07	0.374
85.0	2.97	2.86	0.969	0.339
87.5	2.97	2.86	1.01	0.353
90.0	2.97	2.86	0.811	0.284
92.5	2.97	2.86	0.951	0.332
95.0	2.97	2.86	0.871	0.304
97.5	2.97	2.86	0.815	0.284
100.0	2.97	2.86	0.777	0.272
102.5	2.97	2.86	0.781	0.273
105.0	6.51	2.86	0.749	0.262
107.5	6.51	2.86	0.842	0.294
110.0	6.51	2.86	0.938	0.328
112.5	6.51	2.86	1.06	0.371
115.0	6.51	2.86	1.12	0.392
117.5	6.51	2.86	1.14	0.399
120.0	6.51	2.86	1.19	0.416
125.0	6.51	2.86	1.32	0.462
130.0	6.51	2.86	1.08	0.378

Table 14. Data for 18.6 wt % U-Al

Effective Energy (kev)	X-Ray Control (kvcp)	X-Ray Control (ma)	Copper Filtration (mm)	Counting Rate I With Sample (min^{-1})	Counting Rate I ₀ Without Sample (min^{-1})
40.0	56	10.0	2.86	35,300	71,000
45.0	62	10.0	3.69	44,600	79,200
50.0	66	5.0	4.45	57,200	90,100
55.0	70	5.0	5.52	61,600	90,300
60.0	73	10.0	6.35	67,400	96,900
65.0	83	12.0	9.21	60,500	78,800
70.0	88	12.0	10.8	64,100	80,600
75.0	94	12.5	14.0	63,800	80,000
80.0	98	13.0	15.1	37,700	80,100
85.0	103	12.7	17.5	33,300	66,100
87.5	106	12.5	18.8	36,100	67,800
90.0	110	13.0	20.6	39,700	70,000
92.5	112	12.5	21.6	36,800	64,000
95.0	115	14.0	23.0	42,500	72,100
97.5	118	11.5	24.3	38,100	64,900
100.0	122	10.0	20.3	49,800	78,500
102.5	123	10.5	21.1	51,600	80,600
105.0	126	10.0	22.2	36,000	86,700
107.5	131	10.5	25.4	26,600	72,100
110.0	134	10.5	27.0	22,300	72,300
112.5	137	10.0	28.6	17,200	70,000
115.0	140	12.0	30.2	14,600	67,900
117.5	143	10.0	31.8	11,000	62,600
120.0	149	11.0	33.3	15,800	89,100
125.0	153	10.5	34.9	15,500	85,100
130.0	156	11.0	36.5	17,700	89,700

Table 15. Additional Data and Attenuation Coefficients
for 18.6 wt % U-Al

Effective Energy (kev)	Sample Thickness (mm)	Sample Density (g/cm ³)	μ_l Linear Attenuation Coefficient (cm ⁻¹)	μ_m Mass Attenuation Coefficient (cm ² /g)
40.0	0.754	3.16	9.27	2.93
45.0	0.754	3.16	7.60	2.40
50.0	0.754	3.16	6.02	1.90
55.0	0.754	3.16	5.06	1.60
60.0	0.754	3.16	4.80	1.52
65.0	0.754	3.16	3.50	1.11
70.0	0.754	3.16	3.04	0.962
75.0	0.754	3.16	2.99	0.946
80.0	3.05	3.18	2.47	0.777
85.0	3.05	3.18	2.25	0.708
87.5	3.05	3.18	2.07	0.651
90.0	3.05	3.18	1.87	0.588
92.5	3.05	3.18	1.81	0.569
95.0	3.05	3.18	1.74	0.547
97.5	3.05	3.18	1.75	0.550
100.0	3.05	3.18	1.49	0.468
102.5	3.05	3.18	1.46	0.459
105.0	6.53	3.17	1.35	0.426
107.5	6.53	3.17	1.53	0.483
110.0	6.53	3.17	1.80	0.568
112.5	6.53	3.17	2.15	0.678
115.0	6.53	3.17	2.35	0.741
117.5	6.53	3.17	2.65	0.836
120.0	6.53	3.17	2.65	0.836
125.0	6.53	3.17	2.61	0.823
130.0	6.53	3.17	1.85	0.586

Table 16. Data for 24.8 wt % U-Al

Effective Energy (kev)	X-Ray Control (kvcp)	X-Ray Control (ma.)	Copper Filtration (mm)	Counting Rate I With Sample (min^{-1})	Counting Rate I_0 Without Sample (min^{-1})
40.0	56	10.0	2.86	37,200	71,900
45.0	62	10.0	3.69	50,000	83,200
50.0	66	5.0	4.45	58,000	89,000
55.0	70	5.0	5.52	61,800	89,700
60.0	73	10.0	6.35	67,800	92,000
65.0	83	12.0	9.21	62,800	80,000
70.0	88	12.0	10.8	63,000	77,300
75.0	94	12.5	14.0	65,600	77,700
80.0	98	13.0	15.1	29,900	79,300
85.0	103	12.7	17.5	28,500	67,900
87.5	106	12.5	18.8	29,800	66,400
90.0	110	13.0	20.6	33,400	70,000
92.5	112	12.5	21.6	35,500	71,700
95.0	115	14.0	23.0	36,100	70,000
97.5	118	11.5	24.3	34,800	65,000
100.0	122	10.0	20.3	43,700	77,800
102.5	123	10.5	21.1	46,700	81,100
105.0	126	10.0	22.2	27,200	85,200
107.5	131	10.5	25.4	20,000	71,800
110.0	134	10.5	27.0	16,300	72,100
112.5	137	10.0	28.6	12,000	69,500
115.0	140	12.0	30.2	9,370	66,200
117.5	143	10.0	31.8	6,040	60,400
120.0	149	11.0	33.3	8,240	89,000
125.0	153	10.5	34.9	8,200	85,300
130.0	156	11.0	36.5	10,000	89,000

Table 17. Additional Data and Attenuation Coefficients
for 24.8 wt % U-Al

Effective Energy (kev)	Sample Thickness (mm)	Sample Density (g/cm ³)	μ_p Linear Attenuation Coefficient (cm ⁻¹)	μ_m Mass Attenuation Coefficient (cm ² /g)
40.0	0.508	3.34	12.9	3.86
45.0	0.508	3.34	10.0	2.99
50.0	0.508	3.34	8.42	2.52
55.0	0.508	3.34	7.33	2.19
60.0	0.508	3.34	6.01	1.80
65.0	0.508	3.34	4.76	1.42
70.0	0.508	3.34	4.02	1.20
75.0	0.508	3.34	3.34	1.00
80.0	3.04	3.36	3.21	0.955
85.0	3.04	3.36	2.86	0.851
87.5	3.04	3.36	2.63	0.783
90.0	3.04	3.36	2.44	0.726
92.5	3.04	3.36	2.47	0.735
95.0	3.04	3.36	2.18	0.649
97.5	3.04	3.36	2.05	0.610
100.0	3.04	3.36	1.90	0.565
102.5	3.04	3.36	1.81	0.539
105.0	6.52	3.36	1.75	0.521
107.5	6.52	3.36	1.96	0.583
110.0	6.52	3.36	2.28	0.679
112.5	6.52	3.36	2.70	0.804
115.0	6.52	3.36	2.99	0.890
117.5	6.52	3.36	3.53	1.05
120.0	6.52	3.36	3.67	1.09
125.0	6.52	3.36	3.53	1.05
130.0	6.52	3.36	3.36	1.00

INTERNAL DISTRIBUTION

- | | |
|-------------------------------------|----------------------------------|
| 1. Biology Library | 47. A. L. Lotts |
| 2-4. Central Research Library | 48. H. G. MacPherson |
| 5. Reactor Division Library | 49. R. W. McClung |
| 6-7. ORNL - Y-12 Technical Library | 50. H. F. McDuffie |
| Document Reference Section | 51. W. D. Manly |
| 8-27. Laboratory Records Department | 52. M. M. Martin |
| 28. Laboratory Records, ORNL R.C. | 53. A. M. Perry |
| 29. R. J. Beaver | 54. J. J. Pinajian |
| 30-31. E. P. Blizard | 55. S. A. Rabin |
| 32. J. G. Carter | 56. J. W. Reynolds |
| 33. R. E. Clausing | 57. R. L. Shipp |
| 34. J. E. Cunningham | 58. M. J. Skinner |
| 35. H. W. Dunn | 59. J. A. Swartout |
| 36. J. W. Evans | 60. W. J. Werner |
| 37. B. E. Foster | 61. A. M. Weinberg |
| 38. J. H. Frye, Jr. | 62. R. G. Wymer |
| 39. G. M. Haas | 63. A. A. Burr (consultant) |
| 40-44. M. R. Hill | 64. J. R. Johnson (consultant) |
| 45. L. B. Holland | 65. C. S. Smith (consultant) |
| 46. C. E. Larson | 66. R. Smoluchowski (consultant) |

EXTERNAL DISTRIBUTION

- 67. C. M. Adams, Jr., MIT
- 68-69. D. F. Cope, ORO
- 70. D. E. Baker, GE, Hanford
- 71. Ersel Evans, GE, Hanford
- 72. J. L. Gregg, Cornell University
- 73. J. Simmons, AEC, Washington
- 74. Lawrence M. Slifkin, University of North Carolina
- 75. E. E. Stansbury, University of Tennessee
- 76. D. K. Stevens, AEC, Washington
- 77. Research and Development Division, AEC, ORO
- 78-583. Given distribution as shown in TID-4500 (26th ed.) under Metals, Ceramics, and Materials category